JOC The Journal of Organic Chemistry

ARTICLE

pubs.acs.org/joc

Selective Gold(I)-Catalyzed Formation of Tetracyclic Indolines: A Single Transition Structure and Bifurcations Lead to Multiple Products

Elizabeth L. Noey,[†] Xiang Wang,[‡] and K. N. Houk[*,†]

[†]Department of Chemistry and Biochemistry, University of California, Los Angeles, California 90095, United States

[‡]Department of Chemistry and Biochemistry, University of Colorado, Boulder, Colorado 80309, United States

S *Supporting Information*

ABSTRACT: Several alkynylindoles undergo gold(I)-catalyzed cyclization reactions to form a single isomer in each case. Density functional theory shows why this reaction is favored over the many possible regio- and stereoisomeric reaction pathways. This transformation involves a two-step no-intermediate mechanism with surface bifurcations leading to two or three products. Such bifurcations could explain reactivity in many gold(I)-catalyzed enyne cyclization reactions.

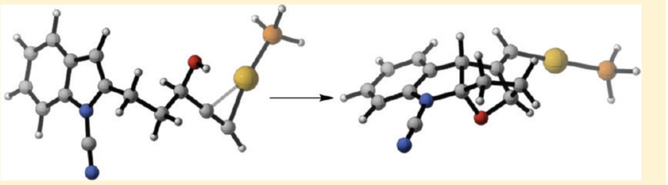

■ INTRODUCTION

Gold(I) complexes are powerful catalysts for the electrophilic activation of alkynes toward a wide range of nucleophiles.[1] These complexes catalyze enyne cyclizations[2] and are more reactive than platinum(II) and other electrophilic metal salts and complexes for this transformation.[2e,h,3] Gold-catalyzed cyclization reactions of alkynes have been shown to take place without the change of gold oxidation state and involve complexes of one or two golds with the alkyne.[4]

Gold(I)-catalyzed cyclizations of enynes, **1**, have been found to give a variety of products, **2**−**8**, depending on the nature of the substituents on the enyne[2] and the ligand on the gold (Scheme 1).[5] Platinum(II) catalysts give similar transformations.[6]

Scheme 1. Products Formed by Transition Metal-Catalyzed Enyne Cyclizations

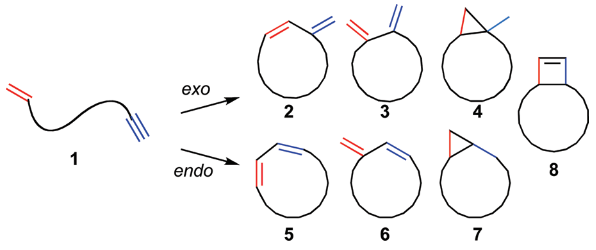

Scheme 2 illustrates how **2** is formed from **1**. First, the gold(I) or platinum(II) catalyst coordinates and activates the alkyne. Prior theoretical studies[2c−f,h,i,n,6a−d,7] suggest that this intermediate can cyclize to form a cyclopropyl metal carbene. The cyclopropyl metal carbene, which has cationic character similar to that of the following structure,[2f,n,6g,12] can open to form the discrete carbocationic intermediate. Other possibilities for this intermediate are to rearrange, be deprotonated and protodemetalated, or undergo nucleophilic attack. Alternatively, the alkyne complex can undergo 6-*exo*-dig cyclization to directly form a carbocationic intermediate. Deprotonation and protodemetalation lead to the product, **2**, regenerating the catalyst.

Scheme 2. Proposed Mechanisms for the Formation of 2 from 1

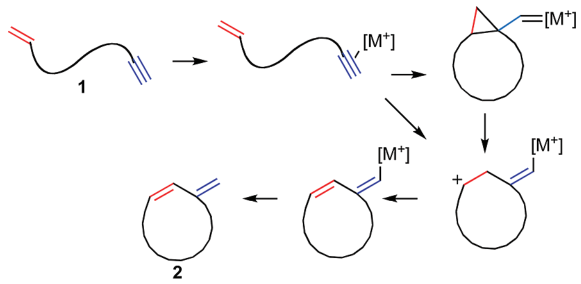

Gold-catalyzed cyclizations of alkynylindoles have previously been studied, and a variety of regio- and stereoisomers are isolated.[2f,g] We have performed a computational study of a very selective reaction of this type. Liu, Xu, and Wang discovered the gold-catalyzed cyclization of the alkynylindole, **9**, shown in eq 1.[8] This reaction could have led to many structural isomers analogous to **2**−**8**, but only **10** is formed. The mechanism proposed for the formation of **10** is shown in Scheme 3. The coordination of the alkyne by the phosphine-gold(I) catalyst (**11**) is followed by nucleophilic attack by the indole, leading to the cyclized intermediate **12**. Intramolecular attack of the alcohol on the iminium and deprotonation leads to the formation of the ether bridge (**13**). Protodemetalation gives the product, **10**, and regenerates the catalyst. Prior studies involving

Received: March 13, 2011
Published: March 23, 2011

Scheme 3. Proposed Mechanism from 9 to 10

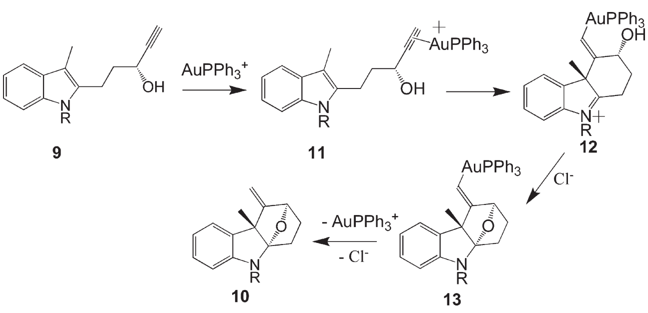

enyne cyclizations of alkynylindoles suggest a different mechanism, in which a spiro intermediate and possibly a cyclopropyl gold carbene intermediate are formed prior to **12**.[2f,g] This conclusion was based on the isolation of a spiro product.

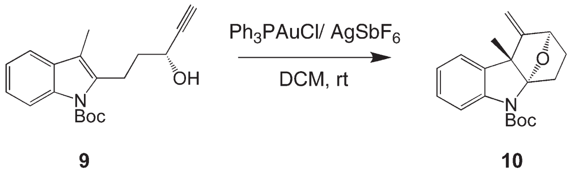

(1)

A series of substrates and catalysts were screened for this transformation. Substitutions at various positions of the indole and of the alkyne were well tolerated. An electron-withdrawing group (EWG) on the indole nitrogen is required for the transformation from **9** to **10**.[8] The EWGs screened include Boc, Ts, and CO_2Me. N-H and N-alkyl systems do not form products analogous to **10**, but instead form a complex mixture of products at higher temperatures.[8] To elucidate the effect of the EWG, we modeled systems with and without EWGs, R = H and CN, respectively. The best catalyst screened for this reaction is PPh_3AuCl with $AgSbF_6$. We modeled the catalyst as $AuPH_3^+$.

We have found that this reaction involves a bifurcating potential energy surface (PES) and is the first example of an enyne cyclization involving this type of surface. On a bifurcating PES, a single transition structure leads to two or more products, because there is a valley-ridge inflection point after the transition structure. This results in two consecutive transition structures with no minimum between them. This type of mechanism has been called a two-step no-intermediate mechanism.[9] Because the intermediates share a common transition structure, the shape of the PES and dynamics control the product distribution.[10a] Bifurcations have been shown to be prevalent in many types of organic reactions and in two other gold(I)-catalyzed processes (Figure 1).[10]

COMPUTATIONAL METHODS

All calculations were performed with Gaussian09[11] with a hybrid density functional (B3LYP) with LANL2DZ and 6-31G(d) basis sets for gold and for all other atoms, respectively. Single point solvation energies were calculated by using the CPCM model for dichloromethane. The possibility that two phosphine−gold(I) catalysts are involved was considered,[4a] but was found to be unlikely. The results with a single phosphine−gold(I) catalyst are presented here. Transition structures **14** and **15**, along with the diastereomeric transition structures, were optimized in the CPCM solution model. Free energy surfaces from **14** and **15** were also computed in the solution model.

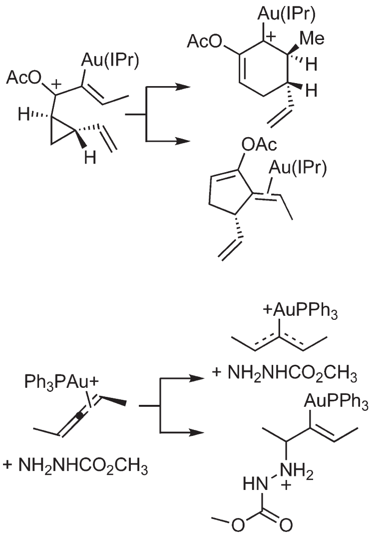

Figure 1. Examples of gold-catalyzed reactions with two-step no-intermediate mechanisms.[10b,c]

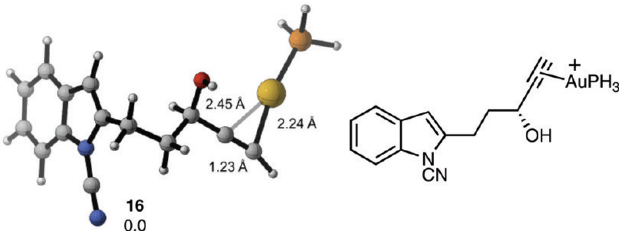

Figure 2. Optimized geometry of **16**, a computational model for **11**. A Chemdraw depiction of the structure is shown to the right.

The origins of the regio- and stereoselectivity have been identified, and a new mechanism for enyne cyclization involving a single transition structure that can form multiple products has been discovered. We describe here our explanation of the selectivity in the transformation from **9** to **10**, and describe surface bifurcations involved in the enyne cyclization step.

RESULTS AND DISCUSSION

Several conformations of the model for the gold(I)−alkyne complex, **11**, were optimized, and the lowest energy conformation was used as the zero of energy (**16**, Figure 2). The complexed C−C bond is polarized such that the terminal carbon is negatively charged and the internal carbon along with the gold and ligand are positive. The triple bond is only moderately lengthened from the uncomplexed triple bond ($\Delta = 0.03$ Å). In agreement with prior gold−alkyne studies,[3b] the gold center is "slipped" to one side of the π bond with alkynyl carbon−gold bond lengths around 2.2 to 2.4 Å.

The gold−alkyne complex can cyclize either by the *exo* (on the alkyne) or *endo* transition structures (**14** and **15**, Figures 3 and 4) The diastereomers of **14** and **15** are **14′** and **15′** and involve attack on the opposite face of the indole (Figure 5).

In an extensive search of the potential energy surfaces, we were surprised to find that there are far fewer saddle points than products, due to bifurcations of reaction paths. These are examples of two-step no-intermediate mechanisms.[9] As shown in Figures 3 and 4, **14** forms **17** and **18** and **15** forms **20**, **21**, and **22**.

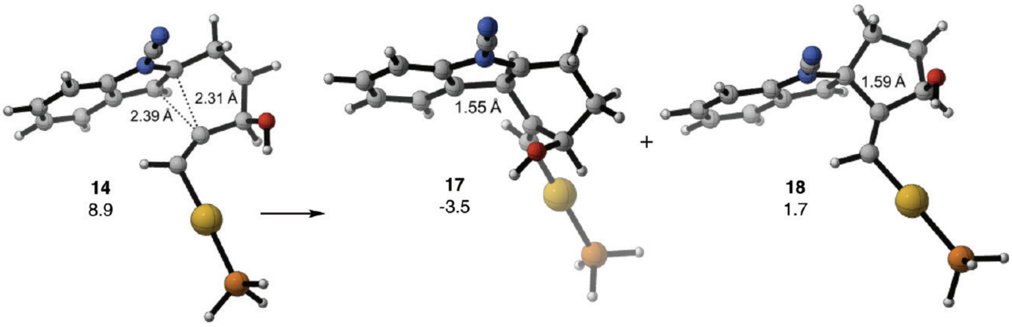

Figure 3. Transition state **14** forms intermediates **17** and **18**. C−C distances are in Å; energies are in kcal/mol.

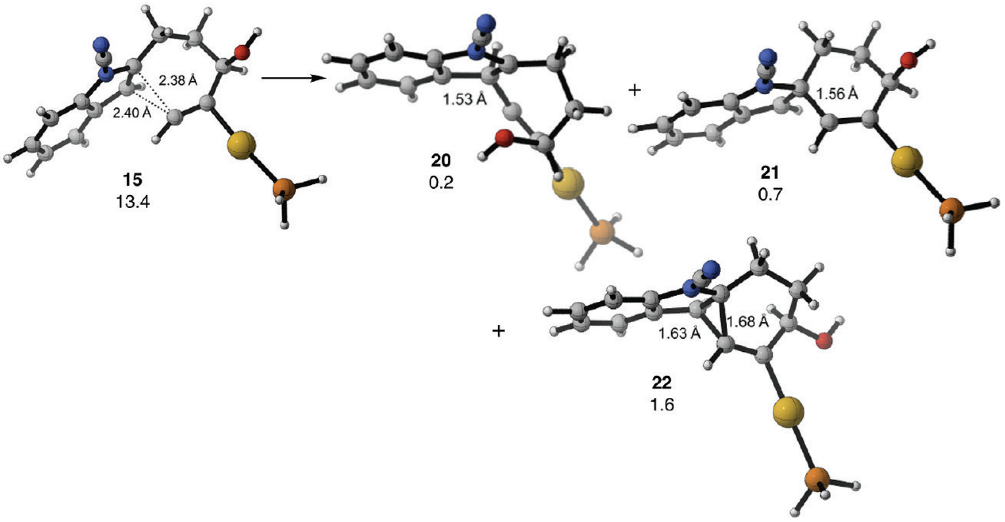

Figure 4. Transition state **15** forms intermediates **20**, **21**, and **22**. C−C distances are in Å; energies are in kcal/mol.

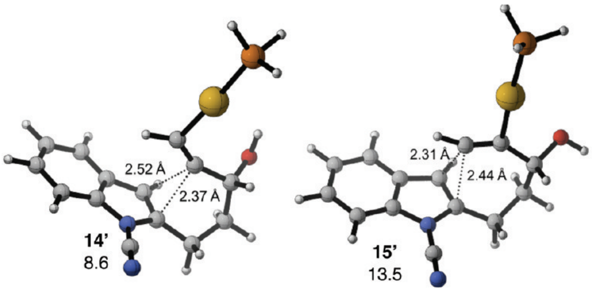

Figure 5. *Exo* (**14′**) and *endo* (**15′**) transition structures. C−C distances are in Å; energies are in kcal/mol.

As shown in Figure 6, transition structure **14** is a saddle point on a very flat surface that leads downhill to intermediates **17** and **18**, which are stabilized iminium and benzyl cations, respectively, and to transition structure **19** between them. Transition structure **19** is only slightly higher in energy than these intermediates, and involves more complete formation of both r_1 and r_2 than transition structure **14**.

The PES from **15** is more complex (Figure 7). In addition to the iminium and benzylic cations (**20** and **22**), a gold-coordinated cyclopropyl carbene intermediate, **21**, is a minimum as well. These structures are shown in Figure 4. This intermediate is not strictly a cyclopropyl metal carbene, because it has carbocationic and carbene character. This is consistent with previous studies on the nature of this type of intermediate.[2f,n,6g,12]

Transition structure **14** and its diastereomer **14′** are 4 to 5 kcal/mol more stable than **15** and **15′**, so that **17**, **17′**, **18**, and **18′** are all formed rapidly. The formation of these intermediates is reversible, with a barrier of 13.4 kcal/mol for the conversion of **17′** back to **16**. Also, the spiro intermediates **18** and **18′** will convert to the more stable **17** and **17′** with a barrier of about 5 kcal/mol.

The cyclization to form the ether bridge is base-promoted. We have explored the reaction involving chloride as a base. Although there is not expected to be a high concentration of chloride in solution due to the addition of $AgSbF_6$, chloride is used because the transition structure for this transformation was not found with other possible bases such as PH_3, H_2O, and OH^-. Because the alcohol must be deprotonated in order to form product, we accept chloride as a model for the base in this transformation. In the transition structures, **23** and **23′**, chloride deprotonates the alcohol as the oxygen attacks C^2 of the indole ring (Figure 8). This transformation is highly favored for **17** but disfavored for **17′**. In structure **17**, C^2 and O are 2.56 Å apart, and in **17′**, they are 3.18 Å apart. Therefore, intermediate **17′** must distort more for the oxygen to be close enough to C^2 to form the ether bridge, so the barrier is higher, and leads to a highly strained intermediate, **24′**. However, the formation of the ether-bridged species **24** from **17** is exothermic by 18.8 kcal/mol. Because transformation from **17** to **24** is highly favored and is not reversible, only **24** is formed. Protodemetalation of **24** (also exothermic) leads to **25** and the regeneration of the gold catalyst. This agrees with experimental data, in which only **10** (which is analogous to **25**) is formed.

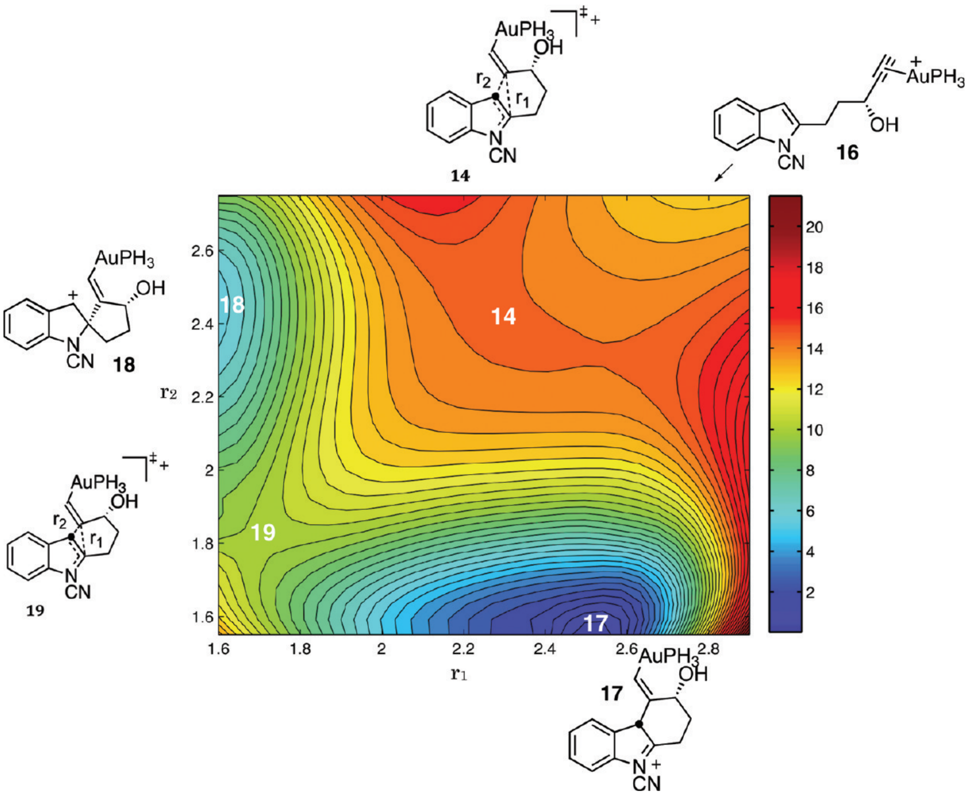

Figure 6. Potential energy surfaces from **16** through transition structure **14** to **17** and **18** calculated with B3LYP/6-31G(d) with the CPCM model in dichloromethane, smoothed with spline interpolation. Energies are in kcal/mol.

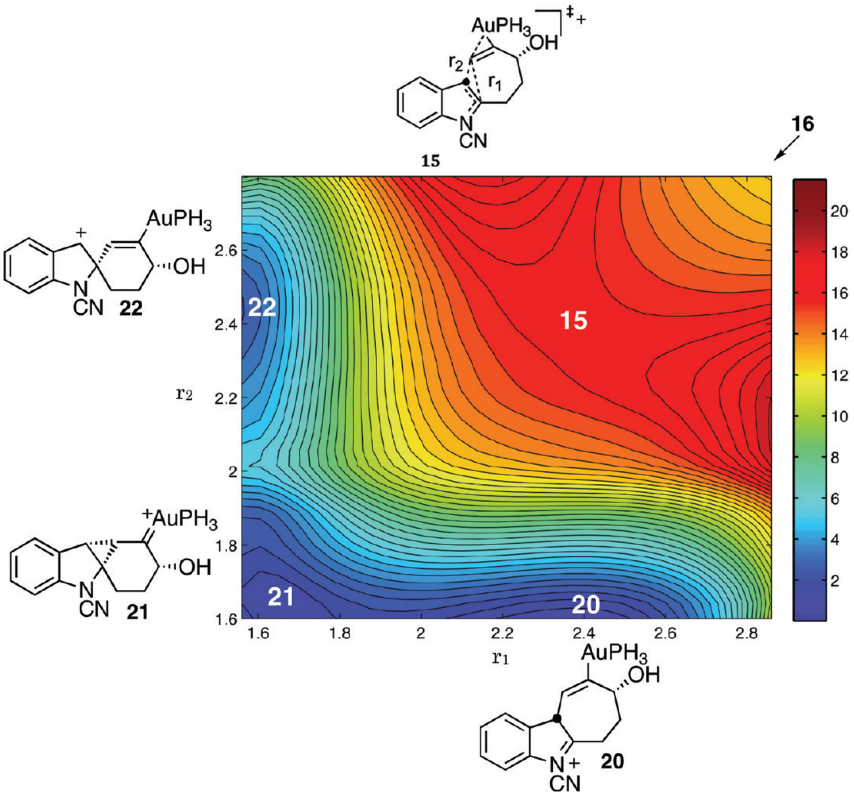

Figure 7. PES from **16** through transition structure **15** to **20**, **21**, and **22**.

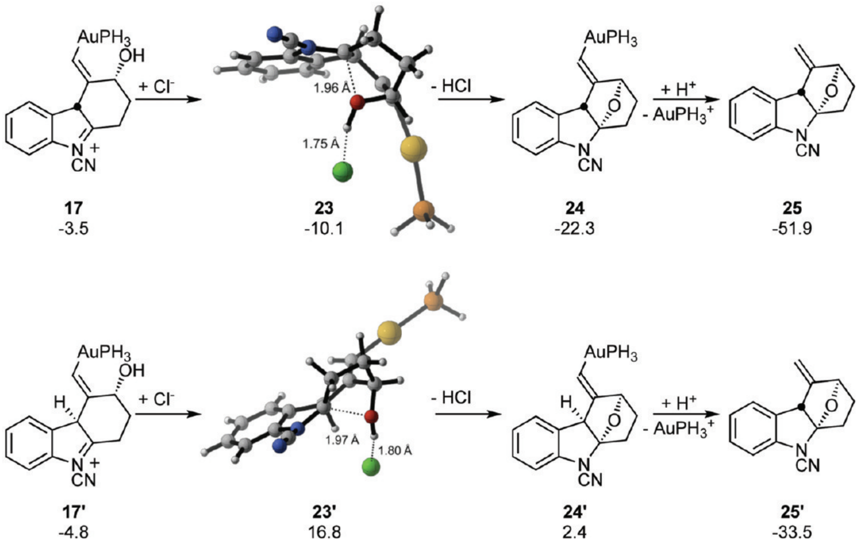

Figure 8. Transformation from **17** and **17′** to the ether-bridged species. Energies are in kcal/mol.

Scheme 4. Free Energy Diagram for the Formation of 25 and Competing Paths[a]

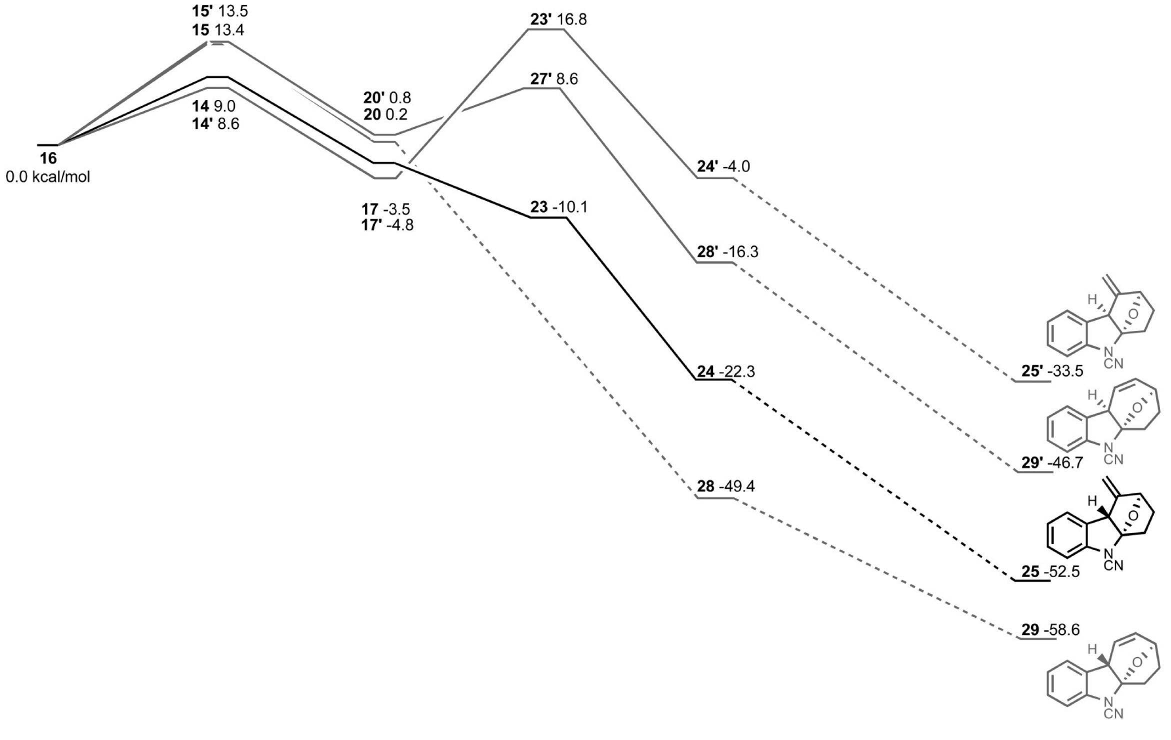

[a] Only the intermediates that lead to ether-bridged products are shown. Higher energy species **18**, **18′**, **21**, **21′**, **22**, and **22′** are not shown for simplicity since they do not lead to cyclized product. The dashed line indicates that no transition state was located for this transformation.

The free energy diagram (Scheme 4) shows the overall transformation from **16** to **25** and potential competing processes. The spiro and cyclopropyl carbene intermediates are not shown, as they do not directly lead to ether-bridged species. The diagram shows that *exo* transition structures **14** and **14′** are lower in energy than the *endo* transition structures **15** and **15′** by about 4 to 5 kcal/mol. Also, the *exo* intermediates formed, **17** and **17′**, are lower in energy than the *endo* intermediates, **20** and **20′**. Intermediate **17′** would form ether-bridged species **24′** through transition structure **23′**. The barrier from **17′** to **24′** (through **23′**) is 21.6 kcal/mol, while the barrier from **17′** back to starting material, **16**, is only 13.4 kcal/mol, so **17′** will revert back to **16**. However, **17** forms the ether-bridged species **24** with no barrier. Because intermediate **17** is cationic and transition state **23** is neutral and our solvation model (CPCM) underestimates the solvation energy of charged species,[13] we expect this barrier to be higher than indicated by our calculations. From **24**, protodemetalation is exothermic and gives the product, **25**.

As indicated above, the competing *endo* cyclizations through **15** and **15′** forming **20** and **20′** are highly disfavored compared to the *exo* cyclizations. The transition structure between **20** and **28**

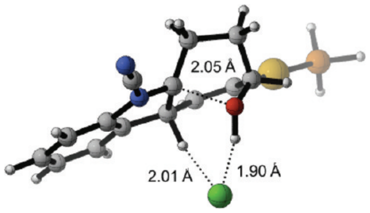

Figure 9. Transition structure **27′**.

was not located, since **20** should not be formed. Interestingly, transition structure **27′** leads to another bifurcation point, such that in **27′** the chloride is positioned to deprotonate the alcohol, or the CH at C^3 (Figure 9). Similar to the comparison between **24** and **24′**, intermediate **28** is lower in energy than **28′**. From **28** and **28′** protodemetalation would lead to **29** and **29′**. Ether-bridged species **29** is the lowest energy species overall but is not formed because of the inaccessibility of **15**.

We also modeled the system with an unsubstituted indole nitrogen (R = H) in order to determine why an EWG is required for the transformation. The model system in which R = H is comparable to the one discussed above, R = CN (Scheme 5). The first cyclization step is more favorable with lower barriers (4 to 9 kcal/mol) and lower energy intermediates (−5 to −20 kcal/mol). This is because the unsubstituted indole is more nucleophilic than the cyano-substituted one and the carbocationic intermediate is more stable due to the absence of the EWG. The second step, in which the alcohol attacks C^2, is greatly disfavored compared to that step in the cyano-substituted system. Here the barrier to cyclization is larger by 7 to 15 kcal/mol; the reactions are now endothermic in all cases except for formation of the ether bridge $\mathbf{28_H}$. Specifically, the cyclization to form the ether bridge from **17** is barrierless ($\Delta G^‡ = -6.6$ kcal/mol) for the cyano-substituted system, while the analogous transformation from $\mathbf{17_H}$ is 8.0 kcal/mol ($\Delta\Delta G^‡ = 14.6$ kcal/mol). It is clear that an EWG is required because it makes C^2 much more electrophilic, thus promoting the second cyclization step. Without the EWG the barrier to cyclization is high and competing processes occur.

CONCLUSION

The regio- and stereoselectivities of the gold-catalyzed indole−alkyne cyclizations of **9** and its analogues have been elucidated, and the effect of the EWG on the indole nitrogen has been determined. The first step of the reaction is selective in that it only allows for the formation of products that go through an *exo* transition structure. Of the intermediates produced, only **17** and **17′** can undergo a second cyclization step to form an ether bridge. In this step the formation of **24** from **17** is far more favorable than the formation of **24′** from **17′**. Thus, due to the trapping of **17** by the second cyclization step, **25** is the only product formed, as found experimentally. The EWG on nitrogen is essential in this reaction, because the formation of the ether bridge is disfavored without it.

For the first time a two-step no-intermediate mechanism has been identified for a transition metal-catalyzed enyne cyclization. This mechanism involves one transition structure that can form up to three products: two different carbocationic species or the gold-coordinated cyclopropyl carbene. This is also the first time a single transition state has been found to lead to three products. Contrary to several other publications[2d,f−j,n,6d,7] on enyne cyclizations, we find that it is not necessary to form the cyclopropyl intermediate in order to obtain the carbocationic species. This

Scheme 5. Free Energy Diagram for the Formation of $\mathbf{25_H}$ and Competing Paths[a]

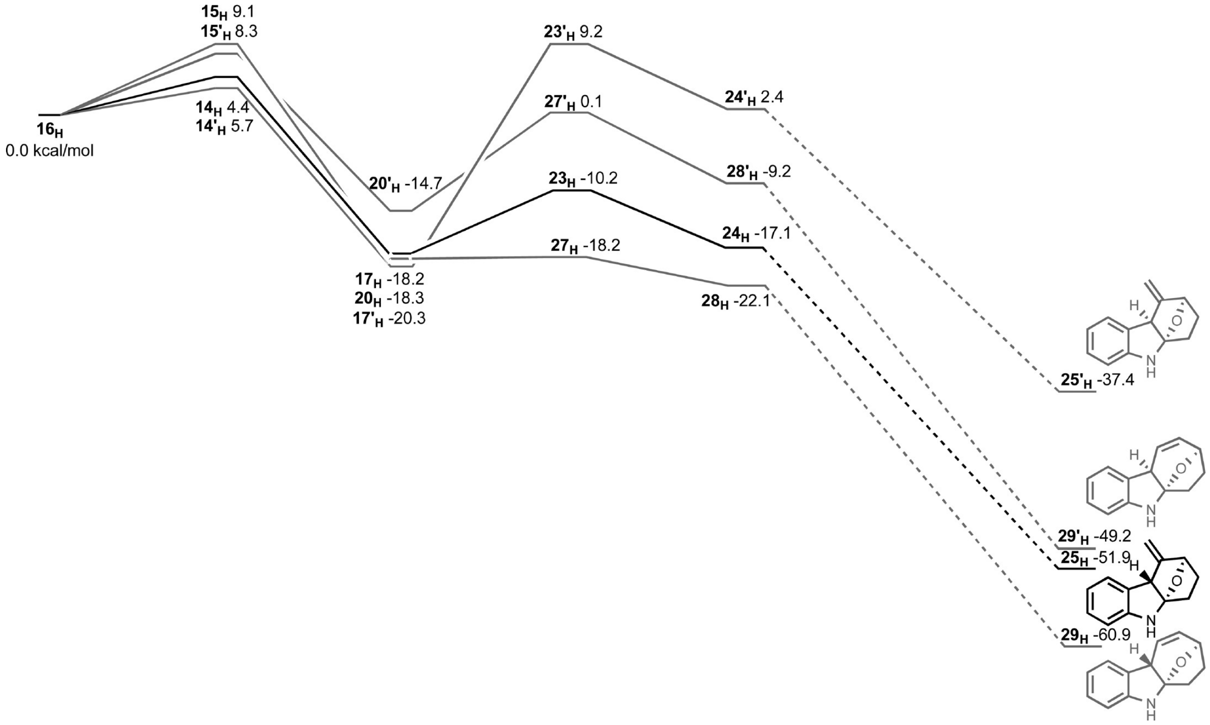

[a] Only the intermediates that lead to ether-bridged products are shown. Species $\mathbf{18_H}$, $\mathbf{18'_H}$, $\mathbf{21_H}$, $\mathbf{21'_H}$, $\mathbf{22_H}$, and $\mathbf{22'_H}$ are not shown for simplicity since they do not lead to cyclized product. The dashed line indicates that no transition state was located for this transformation.

result could have mechanistic implications for a wide range of gold- and platinum-catalyzed reactions.

■ ASSOCIATED CONTENT

Ⓢ Supporting Information. Full ref 11, structures table, energetics, surface scan data points, and Cartesian coordinates. This material is available free of charge via the Internet at http://pubs.acs.org.

■ AUTHOR INFORMATION

Corresponding Author

*E-mail: houk@chem.ucla.edu.

■ ACKNOWLEDGMENT

We are grateful to the National Science Foundation for financial support (CHE-0548209), and to Peng Liu, Paul H.-Y. Cheong, and Robert S. Paton for helpful discussions.

■ REFERENCES

(1) (a) Hashmi, A. S. K. *Gold Bull.* **2003**, *36*, 3. (b) Hashmi, A. S. K. *Gold Bull.* **2004**, *37*, 51. (c) Hoffmann-Röderand, A.; Krause, N. *Org. Biomol. Chem.* **2005**, *3*, 387. (d) Ma, S.; Yu, S.; Gu, Z. *Angew. Chem., Int. Ed.* **2005**, *44*, 200. (e) Hashmi, A. S. K. *Angew. Chem., Int. Ed.* **2005**, *44*, 6990. (f) Li, Z.; Brouwer, C.; He, C. *Chem. Rev.* **2008**, *108*, 3239. (g) Gorin, D. J.; Sjerry, B. D.; Toste, F. D. *Chem. Rev.* **2008**, *108*, 3351. (h) Hashmi, S. K.; Rudolph, M. *Chem. Soc. Rev.* **2008**, *37*, 1766.

(2) (a) Aubert, C.; Buisine, O.; Malacria, M. *Chem. Rev.* **2002**, *102*, 813. (b) Lloyd-Jones, G. C. *Org. Biomol. Chem.* **2003**, *1*, 215. (c) Echavarren, A. M.; Nevado, C. *Chem. Soc. Rev.* **2004**, *33*, 431. (d) Diver S. T.; Giessert, A. J. *Chem. Rev.* **2004**, *104*, 1317. (e) Nieto-Oberhuber, C.; Munoz, M. P.; Bunuel, E.; Nevado, C.; Cárdenas, D. J.; Echavarren, A. M. *Angew. Chem., Int. Ed.* **2004**, *43*, 2402. (f) Soriano, E.; Marco-Contelles, J. *Organometallics* **2006**, *25*, 4542. (g) Ferrer, C.; Echavarren, A. *Angew. Chem.* **2006**, *118*, 1123. (h) Ferrer, C.; Amijs, C.; Echavarren, A. *Chem.—Eur. J.* **2007**, *13*, 1358. (i) Amijs, C. H. M.; Lopez-Carrillo, V.; Raducan, M.; Perez-Galan, P.; Echavarren, A. M. *J. Org. Chem.* **2008**, *73*, 7721. (j) Horino, Y.; Yamamoto, T.; Ueda, K.; Kuroda, S.; Toste, F. D. *J. Am. Chem. Soc.* **2009**, *131*, 2809. (k) Shapiro, N. D.; Toste, F. D. *Synlett* **2010**, *5*, 675. (l) Liu, Y.; Zhang, D.; Zhou, J.; Liu, C. *J. Phys. Chem. A* **2010**, *114*, 6164. (m) Sethofer, S. G.; Mayer, T.; Toste, F. D. *J. Am. Chem. Soc.* **2010**, *132*, 8276. (n) Lopez-Carillo, V.; Echavarren, A. M. *J. Am. Chem. Soc.* **2010**, *132*, 9292.

(3) (a) C. Nieto-Oberhuber, C.; Munoz, M. P.; López, S.; Jimenez-Núñez, E.; Nevado, C.; Herrero-Gomez, E.; Raducan, M.; Echavarren, A. M. *Chem.—Eur. J.* **2006**, *11*, 1677. (b) Sharpio, N. D.; Toste, F. D. *Proc. Natl. Acad. Sci. U.S.A.* **2008**, *105*, 2779.

(4) (a) Cheong, P. H.; Morganelli, P.; Luzung, M. R.; Houk, K. N.; Toste, F. D. *J. Am. Chem. Soc.* **2008**, *130*, 4517. (b) Schmidbaur, H.; Schier, A. *Organometallics* **2010**, *29*, 2.

(5) Benitez, D.; Tkatchouk, E.; Gonzalez, A. Z.; Goddard, W. A.; Toste, F. D. *Org. Lett.* **2009**, *11*, 4798.

(6) (a) Chatani, N.; Kataoka, K.; Murai, S. *J. Am. Chem. Soc.* **1998**, *120*, 9104. (b) Fürstner, A.; Szillat, H.; Stelzer, F. *J. Am. Chem. Soc.* **2000**, *122*, 6785. (c) Fürstner, A.; Stelzer, F.; Szillat, H. *J. Am. Chem. Soc.* **2001**, *123*, 11863. (d) Martin-Matute, B.; Nevado, C.; Cárdenas, D. J.; Echavarren, A. M. *J. Am. Chem. Soc.* **2003**, *125*, 5757. (e) Nevado, C.; Echavarren, A. M. *Chem.—Eur. J.* **2005**, *11*, 3155. (f) Zhang, L.; Sun, J.; Kozmin, S. A. *Adv. Synth. Catal.* **2006**, *348*, 2271. (g) Fürstner, A.; Davies, P. W. *Angew. Chem., Int. Ed.* **2007**, *46*, 3410.

(7) (a) Nieto-Oberhuber, C.; Lopez, S.; Munoz, M. P.; Cardenas, D. J.; Bunuel, E.; Nevado, C.; Echavarren, A. M. *Angew. Chem., Int. Ed.* **2005**, *44*, 6146. (b) Nieto-Oberhuber, C.; López, S.; Muñoz, M. P.; Jiménez-Núñez, E.; Buñuel, E.; Cárdenas, D. J.; Echavarren, A. M. *Chem.—Eur. J.* **2006**, *12*, 1694. (c) Jiménez-Núñez, E.; Echavarren, A. M. *Chem. Commun.* **2007**, 333. (d) Gorin, D. J.; Toste, F. D. *Nat. Rev.* **2007**, *446*, 395. (e) Luzung, M. R.; Mauleon, P.; Toste, F. D. *J. Am. Chem. Soc.* **2007**, *129*, 12402. (f) Soriano, E.; Marco-Contelles, J. *Acc. Chem. Res.* **2009**, *42*, 1026.

(8) Liu, Y.; Xu, W.; Wang, X. *Org. Lett.* **2010**, *12*, 1448.

(9) Singleton, D. A.; Hang, C.; Szymanski, M. J.; Meyer, M. P.; Leach, A. G.; Kuwata, K. T.; Chen, J. S.; Greer, A.; Foote, C. S.; Houk, K. N. *J. Am. Chem. Soc.* **2003**, *125*, 1319.

(10) (a) Ess, D. H.; Wheeler, S. E.; Iafe, R. G.; Xu, L.; Çelebi-Ölçüm, N.; Houk, K. N. *Angew. Chem., Int. Ed.* **2008**, *47*, 7592. Two investigations of Au(I)-catalyzed reactions involving a transition state bifurcation have been reported: (b) Garayalde, D.; Gomez-Bengoa, E.; Huang, X.; Goeke, A.; Nevado, C. *J. Am. Chem. Soc.* **2010**, *132*, 4720. (c) Wang, Z. J.; Benitez, D.; Tkatchouk, E.; Goddard, W. A.; Toste, F. D. *J. Am. Chem. Soc.* **2010**, *132*, 13064.

(11) Frisch, M. J; et al. *Gaussian 09*, revision A.1; Gaussian, Inc.: Wallingford, CT, 2009.

(12) (a) Fürstner, A.; Morency, L. *Angew. Chem., Int. Ed.* **2008**, *47*, 5030. (b) Stephen, A.; Hashmi, K.; Benitez, D. *Angew. Chem., Int. Ed.* **2008**, *47*, 6754. (c) Shapiro, N. D.; Tkatchouk, E.; Wang, Y.; Goddard, W. A.; Toste, F. D. *Nat. Chem.* **2009**, *1*, 482. (d) Seidel, G.; Mynott, R.; Fürstner, A. *Angew. Chem., Int. Ed.* **2009**, *48*, 2510. (e) Perez-Galan, P.; Herrero-Gomez, E.; Hog, D. T.; Martin, N. J. A.; Maseras, F.; Echavarren, A. M. *Chem. Sci.* **2011**, *2*, 141.

(13) Takano, Y.; Houk, K. N. *J. Chem. Theory Comput.* **2005**, *1*, 70.